Thermoelectric figure of merit calculations for semiconducting nanowires

Jane E. Cornett[1] and Oded Rabin[1,2,a)]
[1]*Department of Materials Science and Engineering, University of Maryland, College Park, Maryland 20742, USA*
[2]*Institute for Research in Electronics and Applied Physics, University of Maryland, College Park, Maryland 20742, USA*

(Received 9 March 2011; accepted 12 April 2011; published online 4 May 2011)

A model for the thermoelectric properties of nanowires was used to demonstrate the contrasting influences of quantization and degeneracy on the thermoelectric power factor. The prevailing notion that quantum confinement benefits the thermoelectric power factor is supported by the model when a single-subband dominates transport. When transport involves multiple subbands, the thermoelectric power factor in fact decreases (to ~62% of the bulk value) as the wire radius is initially reduced. This work correctly models the power factor for wire sizes ranging from the nanoscale to bulk and settles the discrepancies between theoretical and measured thermoelectric power factors in nanowires and other nanoscale systems. © *2011 American Institute of Physics*. [doi:10.1063/1.3585659]

The dimensionless thermoelectric figure of merit $ZT=\sigma S^2T/(\kappa_e+\kappa_l)$ of a material is determined by its electrical conductivity σ, Seebeck coefficient S, both the electronic (κ_e) and lattice contributions (κ_l) to its thermal conductivity, and by the absolute temperature T.[1] Prompted by initial theoretical predictions of a vast improvement in ZT of low-dimensional semiconducting structures over bulk,[2,3] a large portion of experimental work in the field of thermoelectrics has been focused on realizing this enhancement via engineering at the nanoscale.[4–6] The predicted increase in ZT is attributed to a simultaneous (1) decrease in κ_l due to increased phonon boundary scattering and lower phonon group velocity and (2) increase in the power factor, $PF=\sigma S^2$, due to the appearance of signatures of quantized energy levels in the density-of-states function—both are the result of confining a material to a nanostructure. The most successful approaches taken recently have concentrated on reducing the thermal conductivity in Bi_2Te_3-based thin-film superlattice devices,[7] PbTe-based quantum dot superlattice structures,[8] bulk nanocomposites of $Bi_xSb_{2-x}Te_3$ [9] and Si_xGe_{1-x},[10] and Si nanowires.[11,12] Though substantial increases in ZT have been realized due to the reduced κ_l of nanoscale systems, improvements in power factor have proven difficult to come by experimentally.[10,13,14] The present work addresses this discrepancy between theory and experiment in the context of semiconducting nanowires.

In 1993, Hicks and Dresselhaus reported ZT calculations for one-dimensional Bi_2Te_3 conductors (i.e., nanowires) assuming a one-subband conduction band.[2] According to this model, the power factor calculated at an optimal doping level follows an approximate r^{-2} dependence, where r is the radius of the cylindrical nanowire (NW)—suggesting that PF can always be improved by decreasing r. Electron transport in most real materials systems cannot be characterized by charge carriers in a single subband—rather, this assumption is only valid for *strongly confined* systems, typically less than 10 nm in critical dimension. For larger structures, multiple subbands contribute to transport. As confinement is weakened (i.e., r increases), the subbands become close in energy, increasing the magnitude of the density-of-states function. Due to its additive effect on the density-of-states, degeneracy of this kind is often utilized as a mechanism for improving thermoelectric efficiency.[14–17] It should be noted that the significance of degeneracy can also be seen in the best *bulk* thermoelectric materials (e.g., SiGe, Bi_2Te_3 systems) which are most often characterized by degenerate carrier pockets. Thus, when multiple subbands are considered high values of the PF are anticipated in NWs both at large and small r due to degeneracy and quantization effects, respectively.

We report room temperature power factor (PF) and figure of merit (ZT) calculations for cylindrical semiconducting NWs. Due to the increasing number of nearly-degenerate states with increasing NW size, calculated PF values exhibit a non-monotonic trend with r. The observed trend is critically different than that predicted by the one-subband model. To verify that in fact this non-monotonic behavior is the direct result of degeneracy, a simplified PF model based on a count of the number of contributing subbands is developed.

The lowest 300 subband energies for each NW radius were determined by solving the Schrödinger equation for electrons confined in a two dimensional infinite potential well with circular boundary conditions.[18] Transport property calculations were performed by solving the Boltzmann transport equation (BTE) as a function of Fermi energy and r.[19] The thermoelectric trends reported here are material-independent, and are intrinsic to changes in the density-of-states function as the result of confinement. Other size and material-dependent effects (primarily carrier pocket multiplicity and changes in the dominant scattering mechanism) can mask the transport phenomena described here, and should therefore be avoided. To capture the physics, we assume a single, spherical electron pocket at the Γ-point and an energy-independent effective relaxation time. We utilize n-type InSb as an example material due to its promise for thermoelectric applications in both bulk and NW form.[20,21] The room temperature electron effective mass ($m_e^*=0.013m_0$) and electron mobility ($\mu_e=70{,}000$ cm^2/V-s) values were obtained from the literature.[22,23]

a)Author to whom correspondence should be addressed. Electronic mail: oded@umd.edu.

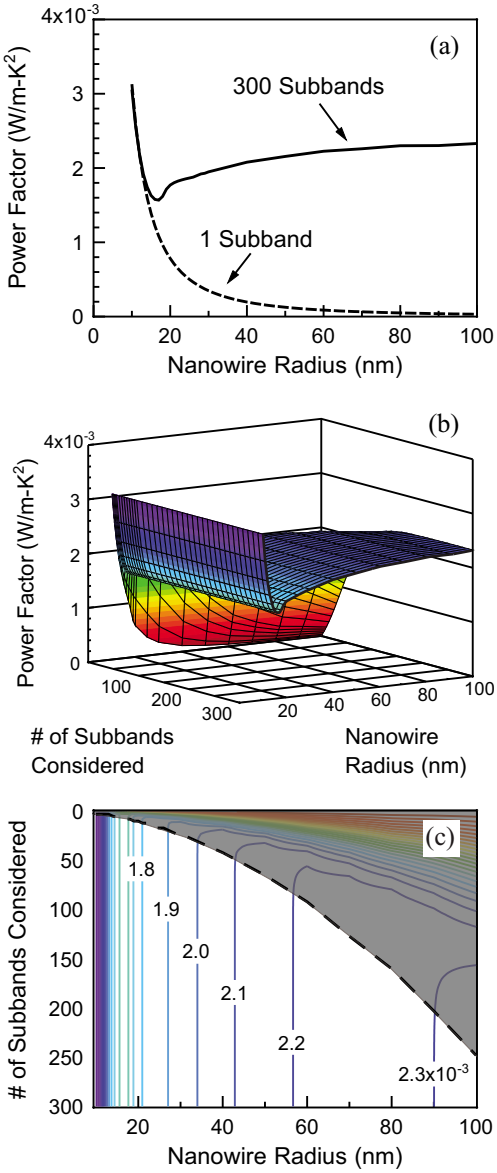

FIG. 1. (Color online) (a) Power factor values calculated as a function of nanowire radius assuming the single-subband model (dashed line) and the many-subband model (solid line). (b) *PF* as a function of both nanowire radius and the number of subbands considered when calculating the transport properties. (c) Contour plot of the *PF* data shown in (b). The spacing between contour lines is 0.1×10^{-3} W/m K^2; some of these lines (between 1.8 and 2.3×10^{-3} W/m K^2) are labeled. The dashed line marks the number of subbands required for convergence of *PF* values as a function of radius. Calculations in the shaded region of the plot are therefore inaccurate. Note that all *PF* values shown reflect an optimal doping level.

Power factor values calculated for InSb NWs considering the conduction band as a single subband are shown in Fig. 1(a). For each radius, the *PF* value corresponds to an optimal Fermi energy (i.e., doping level). This curve demonstrates a r^{-2} dependence, in agreement with the model of Hicks and Dresselhaus.[2] However, when the conduction band constitutes of 300 subbands the calculated *PF* values exhibit very different behavior [Fig. 1(a)]. While the results of the many-subband model exactly match those of the single-subband model in the small-radius limit, the curves diverge as r increases. Down to 17 nm, the *PF* decreases with decreasing radius. Below 17 nm, on the other hand, confinement is significant and *PF* increases with decreasing radius. The *PF* of the NWs can be as little as 62% of the bulk value, which has been calculated as 2.5×10^{-3} W/m-K^2 following the method of Ref. 3. The effect is sizable in NWs with large radii in which the mobility can be safely assumed to be close to its bulk value.[24–27] In InSb NWs, the calculated $ZT(r)$ is a monotonically decreasing function due to the strong dependence of κ_l on radius.[28,29]

The evolution of the *PF* calculations between single-subband and many-subband models is considered in Fig. 1 in which *PF* is plotted as a function of both r and the number of subbands included in the calculations, as a 3D-plot [Fig. 1(b)] and as a contour plot [Fig. 1(c), to aid in the visualization of the data]. Power factor values converge smoothly as the number of subbands is increased from 1 to 300. Models that consider too few subbands in the electronic band structure fail to properly estimate *PF*, particularly for large r. The number of subbands necessary for convergence of the *PF* values ranges from 1 to 250 for the set of NW radii shown here [Fig. 1(c)].

Confidence in the many-subband model is derived from accurate prediction of the bulk *PF* and *ZT* values for InSb. It has long been recognized that the single-subband model vastly underestimates bulk *ZT* values.[2,3] The single-subband *PF* values tend asymptotically to zero with increasing r, far below the experimental bulk value of 2.0×10^{-3} W/m K^2 for n-type InSb.[20] In contrast, large-radius *PF* values obtained with the many-subband model are in good agreement with this value. The authors note that while there has been recent progress in measuring the thermoelectric properties of InSb NWs,[21,30] due to difficulties in controlling impurity doping there are as of yet no experimental *PF* or *ZT* values suitable for comparison with our calculations.

We attribute the non-monotonic trend in the *PF* as a function of NW radius to the opposing contributions of two effects: (1) *discretization* of the electronic energy levels due to strong confinement by the NW boundary, an effect most significant for smaller r and (2) *increased magnitude* of the density-of-states function due to a large number of nearly-degenerate states close to the Fermi energy at large r. The minimum in *PF* versus r therefore indicates opposing contributions of confinement and degeneracy and represents the transition between regions of strong and weak confinement.

A simplified model for estimating the *PF* was developed to confirm that degeneracy is indeed the source of the observed increase in *PF* with radius. We approximate $PF(r)$ as the product of the power factor calculated for a single subband system $[PF_{1\text{-band}}(r)]$ and the number of nearly-degenerate subbands $[\tilde{N}(r)]$. $\tilde{N}$ is essentially a count of the number of subbands contributing to transport. For N degenerate subbands, the simple identity $PF(r)=N\times PF_{1\text{-band}}(r)$ holds. For subbands not exactly equal in energy, the approach is slightly more complicated: A weight factor ranging between 0 and 1 is assigned to each subband, depending only on its energy relative to the Fermi energy (E_f). The weight function is based on the electron occupancies of the subbands. Subbands close to E_f are counted as 1, while the weight function falls off for subbands increasingly higher in energy. For each radius, $\tilde{N}$ is the sum over the weights of all subbands, and is finite. As anticipated, $\tilde{N}(r)$ increases monotonically between radii of 10 and 100 nm [inset of Fig. 2]. This trend confirms that while a single-subband model may be a valid approximation for small r, the same does not hold

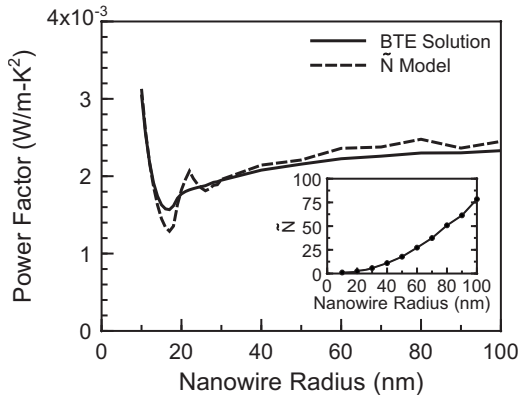

FIG. 2. Power factor as a function of radius calculated by solving the BTE with the complete band structure (solid line) and calculated assuming a simple model based on a count of the number of contributing subbands, $\tilde{N}$ (dashed line). The inset shows calculated $\tilde{N}$ values as a function of nanowire radius.

true for large radii. Multiplying $\tilde{N}(r)$, a monotonically increasing function of r, by $PF_{1\text{-band}}(r)$, exhibiting an r^{-2} dependence, results in the dashed line in Fig. 2 which accurately predicts a minimum PF at $r=17$ nm. Despite the minimal computational effort required by this simple model, excellent agreement is seen with the PF values calculated using the BTE [Fig. 1, and solid line in Fig. 2]. Discrepancies between the simple $\tilde{N}$ model and full BTE calculations may be attributed to (1) uncertainty in determining the optimal Fermi energy for each r and (2) overestimation of the contribution of subbands far below the Fermi energy (an error that becomes more significant with increasing r). The power of this simplified model in estimating PF values, based solely on the count of the number of subbands contributing to transport, leads us to conclude that degeneracy plays a dominant and beneficial role in thermoelectric transport, particularly when energy quantization is small.

The reduced density-of-states in NW systems and its detrimental effect on the thermoelectric power factor have not been discussed in the literature, though several mechanisms leading to a comparable decrease in the PF in NWs have been identified in the past. A related mechanism is the lifting of carrier pocket degeneracy due to quantization—however, this is a material-specific phenomenon that imposes conditions on the band structure of the material and the crystallographic orientation of the NW. A decrease in carrier mobility with confinement can also have an unfavorable effect on the thermoelectric properties.[31] This mechanism is most effective at remarkably small radii ($r<10$ nm) where single-subband conditions apply. The nonmonotonic behavior shown here is not material-specific, and is predicted for *any individual carrier pocket.* The effect is pronounced in weakly confined electronic systems, corresponding to the size range of most experimental NW systems that can be reproducibly fabricated today ($r>10$ nm).

In summary, we have reported a non-monotonic dependence of the power factor on NW radius for n-type InSb NWs. This behavior is attributed to the increasing number of nearly-degenerate subbands with r, a hypothesis supported by the results of a model based on a weighted count of the subbands that contribute to transport. This phenomenon is not exclusive to InSb—rather, it may explain why for many conventional thermoelectric materials the improvement in PF when moving from bulk to nanoscale has proven to be so elusive. With the assumption of a radius-dependent lattice thermal conductivity, the expected monotonic trend in $ZT(r)$ is recovered. It is important to note, however, that electron and hole transport in semiconductors is dependent on specific materials parameters (i.e., effective mass, mobility, degeneracy of carriers). Thermoelectric systems in which multiple carrier types are found (including p-type InSb) will likely exhibit more complex radius-dependent behavior.

This work was supported by the Minta Martin Foundation.

[1]F. J. DiSalvo, Science **285**, 703 (1999).
[2]L. D. Hicks and M. S. Dresselhaus, Phys. Rev. B **47**, 16631 (1993).
[3]L. D. Hicks and M. S. Dresselhaus, Phys. Rev. B **47**, 12727 (1993).
[4]G. Chen, M. S. Dresselhaus, G. Dresselhaus, J. P. Fleurial, and T. Caillat, Int. Mater. Rev. **48**, 45 (2003).
[5]M. S. Dresselhaus, G. Chen, M. Y. Tang, R. G. Yang, H. Lee, D. Z. Wang, Z. F. Ren, J. P. Fleurial, and P. Gogna, Adv. Mater. (Weinheim, Ger.) **19**, 1043 (2007).
[6]Y. Lan, A. J. Minnich, G. Chen, and Z. Ren, Adv. Funct. Mater. **20**, 357 (2010).
[7]I. Chowdhury, R. Prasher, K. Lofgreen, G. Chrysler, S. Narasimhan, R. Mahajan, D. Koester, R. Alley, and R. Venkatasubramanian, Nat. Nanotechnol. **4**, 235 (2009).
[8]T. C. Harman, M. P. Walsh, B. E. LaForge, and G. W. Turner, J. Electron. Mater. **34**, L19 (2005).
[9]B. Poudel, Q. Hao, Y. Ma, Y. Lan, A. Minnich, B. Yu, X. Yan, D. Wang, A. Muto, D. Vashaee, X. Chen, J. Liu, M. S. Dresselhaus, G. Chen, and Z. Ren, Science **320**, 634 (2008).
[10]G. Joshi, H. Lee, Y. Lan, X. Wang, G. Zhu, D. Wang, R. W. Gould, D. C. Cuff, M. Y. Tang, M. S. Dresselhaus, G. Chen, and Z. Ren, Nano Lett. **8**, 4670 (2008).
[11]A. I. Boukai, Y. Bunimovich, J. Tahir-Kheli, J.-K. Yu, W. A. Goddard III, and J. R. Heath, Nature (London) **451**, 168 (2008).
[12]A. I. Hochbaum, R. Chen, R. D. Delgado, W. Liang, E. C. Garnett, M. Najarian, A. Majumdar, and P. Yang, Nature (London) **451**, 163 (2008).
[13]T. C. Harman, D. L. Spears, and M. J. Manfra, J. Electron. Mater. **25**, 1121 (1996).
[14]C. M. Jaworski, V. Kulbachinskii, and J. P. Heremans, Phys. Rev. B **80**, 233201 (2009).
[15]O. Rabin, Y.-M. Lin, and M. S. Dresselhaus, Appl. Phys. Lett. **79**, 81 (2001).
[16]D. A. Broido and T. L. Reinecke, Appl. Phys. Lett. **70**, 2834 (1997).
[17]J. P. Heremans, V. Jovovic, E. S. Toberer, A. Saramat, K. Kurosaki, A. Charoenphakdee, S. Yamanaka, and G. Jeffrey Snyder, Science **321**, 554 (2008).
[18]Y.-M. Lin, M.Sc. thesis, Massachusetts Institute of Technology, 2000.
[19]N. W. Ashcroft and N. D. Mermin, *Solid State Physics* (Holt, Rinehart and Winston, New York, 1976).
[20]S. Yamaguchi, T. Matsumoto, J. Yamazaki, N. Kaiwa, and A. Yamamoto, Appl. Phys. Lett. **87**, 201902 (2005).
[21]F. Zhou, A. L. Moore, M. T. Pettes, Y. Lee, J. H. Seol, Q. L. Ye, L. Rabenberg, and L. Shi, J. Phys. D **43**, 025406 (2010).
[22]R. A. Stradling and R. A. Wood, J. Phys C: Solid State **3**, L94 (1970).
[23]O. Madelung, *Semiconductors: Group IV Elements and III-V Compounds* (Springer, Heidelberg, 1991).
[24]M. S. P. Lucas, J. Appl. Phys. **36**, 1632 (1965).
[25]K. Fuchs, Math. Proc. Cambridge **34**, 100 (1938).
[26]E. H. Sondheimer, Adv. Phys. **1**, 1 (1952).
[27]O. Gunawan, L. Sekaric, A. Majumdar, M. Rooks, J. Appenzeller, J. W. Sleight, S. Guha, and W. Haensch, Nano Lett. **8**, 1566 (2008).
[28]N. Mingo and D. A. Broido, Phys. Rev. Lett. **93**, 246106 (2004).
[29]See supplementary material at http://dx.doi.org/10.1063/1.3585659 for calculated ZT as a function of nanowire radius.
[30]J. H. Seol, A. L. Moore, S. K. Saha, F. Zhou, L. Shi, Q. L. Ye, R. Scheffler, N. Mingo, and T. Yamada, J. Appl. Phys. **101**, 023706 (2007).
[31]D. A. Broido and T. L. Reinecke, Phys. Rev. B **64**, 045324 (2001).